First-principles study of the electronic properties of simple hexagonal graphite

J.-C. Charlier and J.-P. Michenaud
Laboratoire de Physico-Chimie et de Physique des Matériaux, Université Catholique de Louvain, 1 Place Croix du Sud, B-1348 Louvain-La-Neuve, Belgium

X. Gonze
Cornell University, Clark Hall, Ithaca, New York 14850
(Received 25 November 1991; revised manuscript received 26 February 1992)

The electronic properties of simple hexagonal graphite have been studied in the framework of the density-functional technique, using nonlocal ionic pseudopotentials and a large number of plane waves. This work leads to a first-step qualitative understanding of the electronic properties of nonperiodic structures such as pregraphitic and disordered carbons (turbostratic graphite), which are composed of periodic regions of simple hexagonal graphite surrounded by domains of the usual (Bernal) form of graphite. Particular attention has been paid to the comparison with the properties of the Bernal graphite. The valence charge density, the density of states, the band structure, as well as a description of the electronic energies at the Fermi level are provided. The latter is parametrized by a *tight-binding* model, and compared to the Slonczewski-Weiss-McClure model of Bernal graphite electronic energies. The Fermi surface is calculated and an exchange of hole and electron pockets between these two forms of graphite is observed. The behavior of electronic energies under pressure, and the associated deformation potentials, are also studied.

I. INTRODUCTION

At ordinary temperature and pressure, the stable form of carbon is graphite, a semimetallic solid that has been extensively studied,[1-4] due to its technological importance as well as its archetypal bidimensional properties.[5] There is also considerable interest in the weak binding between layers, ascribed to be van der Waals forces. The nature of the interlayer bonding is of particular importance for the study of graphite intercalation compounds (GIC).

Graphite crystal structure consists of carbon atoms arranged in planar hexagonal networks. In general, these layers adopt an *ABAB*... stacking sequence (Bernal structure[6]), half the atoms lying directly above those in adjacent planes and half lying above the centers of the hexagons in the adjacent planes. Crystalline (natural and synthesized) graphite is a mixture of Bernal and rhombohedral graphite (where the layers are stacked in an *ABCABC* fashion), in the following ratio: 80% Bernal, 14% rhombohedral, and 6% disordered.[7] In GIC's, the carbon layers can be stacked in different ways, either similar to the Bernal structure (*ABAB*... stacking) or with layers of carbon atoms located directly on top of each other (*AAA*... stacking). Such is the case for the different stages of Li intercalated graphite (LiC_n).[8] These two modifications of graphite are presented in Fig. 1. The configuration of simple hexagonal graphite, where the carbon atoms in consecutive layers are directly above each other, has not been observed in crystalline graphite but in disordered or pregraphitic carbon usually called "turbostratic" graphite[9] as we shall mention later.

All previous *ab initio* calculations involving graphite focused on the structural and electronic properties of Bernal or rhombohedral structure.[4,10,11] In this paper, we aim at presenting state-of-the-art *ab initio* calculations of a whole set of electronic properties of simple hexagonal graphite: valence charge density, band structure, density of states (DOS), and the Fermi surface.

The behavior of the electronic energies under pressure simulated by a variation of the graphitic interlayer distance (<1.35 Å) and the associated deformation potentials are also calculated self-consistently. Within the bounds of possibility, these electronic properties are related to the *tight-binding* models established for the Bernal graphite [Slonczewski-Weiss-McClure (SWMcC) model][2]

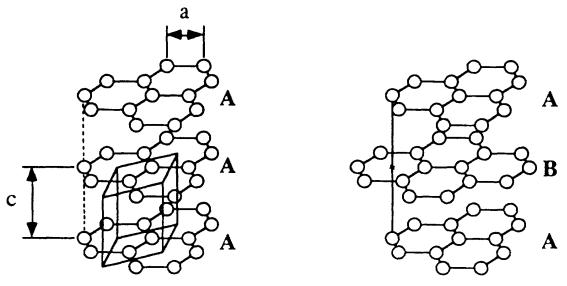

FIG. 1. Comparison between two different graphitic stackings: simple hexagonal graphite and natural hexagonal graphite (Bernal structure). They differ in the shift of the middle plane in the *ABAB* stacking (all the planes are directly above each other in the *AAA* stacking). The unit cell of the simple hexagonal crystalline structure is also shown. The interlayer distance is *c* and the distance between nearest neighbors is *a*.

and for the simple hexagonal graphite,[12] which parametrize the band structure around the Fermi level.

The paper starts with a presentation of the graphitic structure and a brief discussion of the *ab initio* theoretical method we used to study the above-mentioned properties (Sec. II): a self-consistent density-functional approach, using *ab initio* nonlocal ionic pseudopotentials and a local-density approximation for exchange and correlation. Numerical results for the electronic properties and Fermi surface description are presented and compared with the corresponding results of the Bernal structure in Secs. III and IV. Finally, we summarize this study.

Our comparative studies of two allotropic forms of graphite (hypothetical $AAA\ldots$ stacking and Bernal structure) is a first step for the qualitative resolution of the electronic properties of the already mentioned turbostratic graphite,[13] disordered graphite without any periodicity in the z direction (perpendicular to the planes of hexagonally arranged carbon atoms) and which is composed of alternative sequences of $AAA\ldots$ and $ABAB\ldots$ stackings. This study can also stimulate future experimental work relative to the electronic properties of GIC specially in providing *ab initio* values to the atomic interaction parameters which could be used in a rigid-band model. The effect of the stacking on the physical properties of graphites could also be helpful in the study of fullerenes.[14]

II. ATOMIC STRUCTURE AND THEORETICAL METHOD

The unit cell of the simple hexagonal graphitic lattice is shown in Fig. 1. The tridimensional structure of simple hexagonal graphite is a simple stacking of planes noted AAA, indicating that all the planes have the same projections on the xy plane (cf. Fig. 1). This crystallographic structure belongs to the $P6/mmm$ space group. Two atoms are present in the three-dimensional unit cell. This latter is nearly half the volume of the unit cell of the Bernal structure which contains four atoms. At 0 K, the distance between nearest neighbors is $a = 1.420$ Å and the interlayer separation is $c = 3.335$ Å. These values have been calculated *ab initio* by minimizing the total energy, as obtained by the theoretical method, of which we now give a short discussion.

A longer description can be found in Ref. 4, where it was used for the study of Bernal graphite. Briefly, we performed a quite standard Hohenberg-Kohn-Sham density-functional calculation[15] with the Ceperley-Alder exchange-correlation energy as parametrized by Perdew and Zunger.[16]

We used a plane-wave basis set (up to 1700 plane waves, depending on the required accuracy) within the framework of the momentum-space formalism.[17] The ionic core potential was replaced by an *ab initio* norm-conserving pseudopotential, different from the carbon pseudopotential extracted from the complete table of Bachelet, Hamann, and Schlüter,[18] that was used in Ref. 4. The new pseudopotential is softer than the one found in Ref. 18, and was constructed using the same procedure, but with different "cc_l parameters": 1.8 ($l=0$), 2.0 ($l=1$), and 3.5 ($l=2$). The transferability of this pseudopotential has been tested. As in the Bernal graphite study,[4] we carefully checked the Brillouin-zone sampling and the treatment of the charge transfer from valence to conduction bands (semimetallicity), in order to get maximum truncation error on energies at the Fermi level on the order of 5 meV.

III. THE ELECTRONIC PROPERTIES

In graphite, the spacing between layers is large compared with the C—C bond-length distance in the layers. The strong bonding (angles of 120° between the segments connecting nearest-neighbor atoms) within the layers (intralayer) is described by sp^2 hybridized $2s$, $2p_x$, and $2p_y$ atomic orbitals (σ states), and the weak interlayer bonding is derived from the overlap between $2p_z$ orbitals (π states) perpendicular to the graphitic planes. The resulting band structure consists of bonding π and σ states and antibonding π^* and σ^* states forming the valence and conduction bands, respectively. Semiempirical as well as *ab initio* calculations[4,11] have demonstrated the essentially two-dimensional (2D) character of graphite by predicting little or no dispersion of the σ bands perpendicular to the basal planes although the π bands show some c-axis dispersion. The weak interactions between graphitic planes modify the ideal 2D situation which leads to a zero-gap semiconductor,[1] and create a semimetal.

A. The valence charge density

In order to get the self-consistent valence density, 995 plane waves and 28 special points (14 k points in each plane, with two planes) have been used. This set of plane waves corresponds to a kinetic energy of 32 hartrees.

The isodensity lines are presented in Fig. 2. They

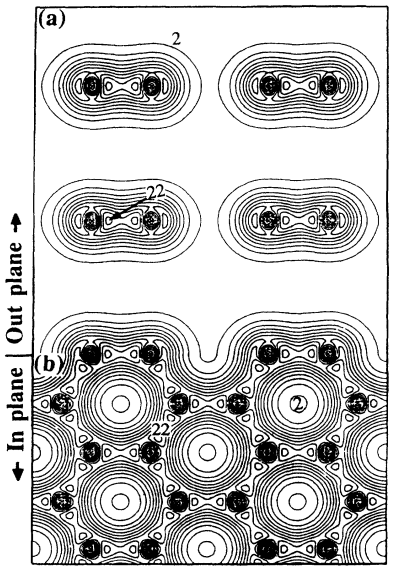

FIG. 2. Valence electron pseudocharge density of simple hexagonal graphite obtained *ab initio*. (a) Perpendicular to graphitic planes (110), (b) in the graphitic plane (001). The contour interval is in units of 0.1 electrons/Å^3 with a difference of 0.2 electrons/Å^3 between curves. Crosses indicate atoms positions.

display the main features of binding: the absence of covalent bonds in the (110) plane perpendicular to the graphitic layers [Fig. 2(a)] and the covalent bonds between carbon atoms in the (001) plane [Fig. 2(b)]. The hexagonal symmetry is shown in the in-plane density while the c-axis density exhibits the absence of shift between neighboring planes in the stacking. The anisotropy of such a crystal is obvious.

B. The band structure

The band structures of simple hexagonal graphite and Bernal structure, dominated by the two-dimensional in-plane interactions, are expected to be nearly identical. The main features of the energy bands of graphite are directly obtained within a good accuracy using a two-dimensional calculation, except for the energy range close to the Fermi energy (ε_F). The electronic and transport properties are dominated by this region where the two structures differ significantly from each other. The aim of the next section will be to find these important differences in the π bands close to the Fermi energy.

The self-consistent calculation of the density of charge allows us to construct the Kohn-Sham band structure. The identification of this band structure with the quasiparticle (experimental) band structure was discussed in the Bernal graphite study.[4] Figure 3(a) shows the band structure of simple hexagonal graphite in different special directions of the Brillouin zone[19] (for the first four or five bands). This band structure is compared to the band structure of Bernal graphite [cf. Fig. 3(b)].

We now discuss these two band structures with respect to the 2D graphite monolayer band structure. The 3D weak interplanar bonding leaves the latter practically unchanged, except for weak dispersion along the direction perpendicular to the graphitic planes. Moreover, the simple hexagonal graphite and the graphite monolayer unit cells have the same number of carbon atoms. However, in the Bernal case, each band of the bidimensional structure is split in two bands because of the doubling of the unit cell. In the AHL plane of the Brillouin zone of this structure, the tridimensional structure is very similar to the monolayer band structure or to the simple hexagonal graphite case. The crystallographic structure possesses a twofold screw axis normal to the zone boundary plane[20] imposing the degeneracy not to be lifted to any order over that entire plane. By contrast, the middle plane ΓMK of the Brillouin zone of Bernal graphite does not possess such a particular reversal element and some degeneracies are lifted. This lift of the degeneracy is nearly invisible in Fig. 3(b), but lines KH, ΓK, and ML show some more strongly lifted degeneracies. At the Γ point, the dispersion of the π bands (third and fourth valence bands) is also very strong. Table I focuses on the numerical results for energy differences of simple hexagonal graphite and Bernal graphite (theoretical and experimental ones) while energies around the Fermi level will be studied in the next section.

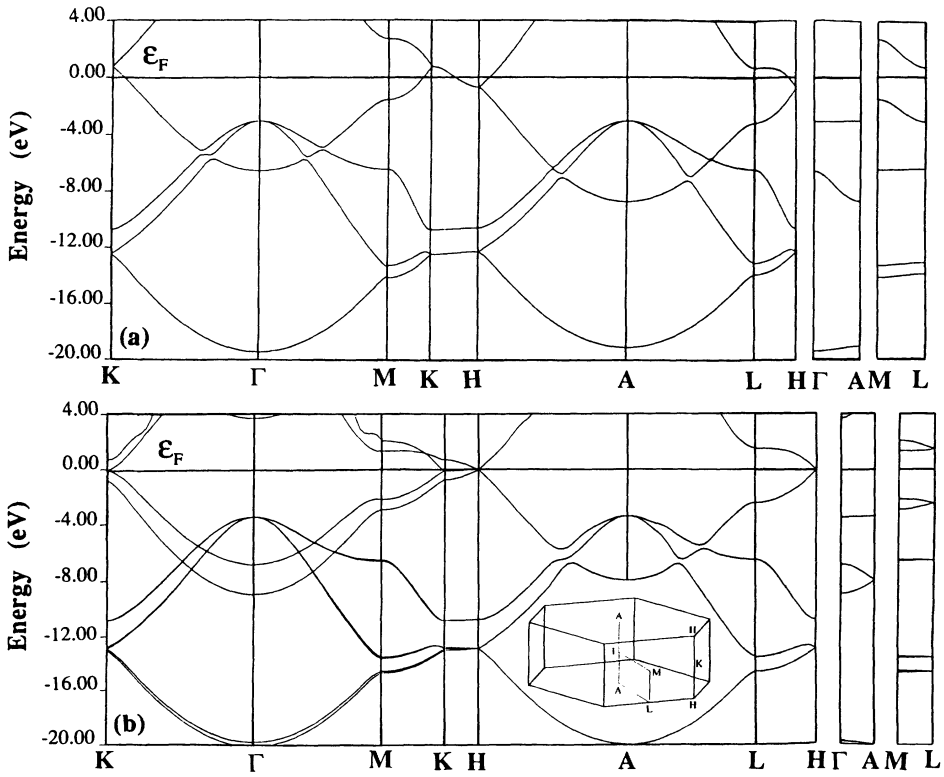

FIG. 3. *Ab initio* band structures of simple hexagonal graphite (a) and natural graphite (b) along different lines in the Brillouin zone, shown in the inset. The usual Bouckaert-Smoluchowski-Wigner (Ref. 19) notations are used.

TABLE I. Characteristic electronic energies (in eV) of simple hexagonal graphite and Bernal structure evaluated from the Fermi level. The first two columns are theoretical results. The last column is a collection of experimental data relative to natural graphite.

	AAA theoretical		*ABAB* theoretical	*ABAB* experimental
Bottom σ	-19.5^a		-19.8^b	
			-20.1^b	-20.6^c
Bottom π	-6.6^a		-6.8^b	$-7.2,^c -6.6,^d -5.7^e$
			-8.9^b	$-8.1,^c -8.5^d$
Top σ	-3.1^a		-3.5^b	$-4.6,^c -5.5^d$
			-3.4^b	
Unoccupied σ^*	3.9^a		3.7^b	
	8.2^a		7.9^b	6.9^c
			7.9^b	
π bands at point K and at point H				
$E_K - E_{KH/2}$	0.78^a	$\varepsilon_1 - \varepsilon_c$	0.80^b	0.72^f
$E_{KH/2} - E_H$	0.67^a	$\varepsilon_3 - \varepsilon_2$	0.86^b	0.84^f

[a]Present work.
[b]Reference 4.
[c]W. Eberhardt, J. T. McGovern, E. W. Plummer, and J. E. Fischer, Phys. Rev. Lett. **44**, 200 (1980).
[d]A. R. Law, J. J. Barry, and H. P. Hughes, Phys. Rev. B **28**, 5332 (1983).
[e]A. Bianconi, S. B. M. Hagström, and R. Z. Bachrach, Phys. Rev. B **16**, 5543 (1977).
[f]G. Bellodi, A. Borghesi, G. Guizzeti, L. Nosenzo, E. Reguzzoni, and G. Sammoggia, Phys. Rev. B **12**, 5951 (1975).

In general, the present results are consistent with the numerical values also obtained for the Bernal structure. The effect of the stacking on the main features of the band structures is very weak. The degeneracy of the bands between the K point and the H point of the Brillouin zone near the Fermi level is in good agreement with the *tight-binding* study established for this particular stacking.[12] The total valence-band width (19.5 eV), the σ-band width (16.4 eV), and the σ-π band separations [12.9 eV (bottom) and 3.5 eV (top)] are very close to the calculations obtained for Bernal graphite.

C. The density of states

The electronic DOS, as a function of the energy, has been calculated with the tetrahedron method,[21] using 198 k points in the Brillouin zone (three planes of 66 k points) and a kinetic energy of 36 hartrees associated to the set of plane waves. The calculated DOS for the valence states of simple hexagonal graphite and its 0.5-eV Gaussian convolution are presented in Figs. 4(a) and 4(b), respectively.

The bidimensional characteristic of the first σ bands, which had already been seen in the lack of dispersion of the Γ-A, M-L, and K-H lines in the band structure, is confirmed by the typical step function which appears in the DOS form. This feature is also present in the Bernal graphite whose DOS is rather similar to the present one.[4]

IV. THE FERMI SURFACE

A. Tight-binding model

The interactions between graphitic planes are clearly weaker than the interactions inside the plane. The bidimensional interactions only lead to a zero-gap semiconductor with linear dispersion relations at the Fermi level near the K point.[1]

In a previous paper,[12] we have parametrized the band structure of simple hexagonal graphite at the Fermi level using a *tight-binding* method. The electronic energy spectrum near this energy can be described by four parameters, α_0, α_1, α_2, and α_3, which define the interaction energies between π orbitals (the σ orbitals do not contribute to the level occupation near the Fermi energy) from

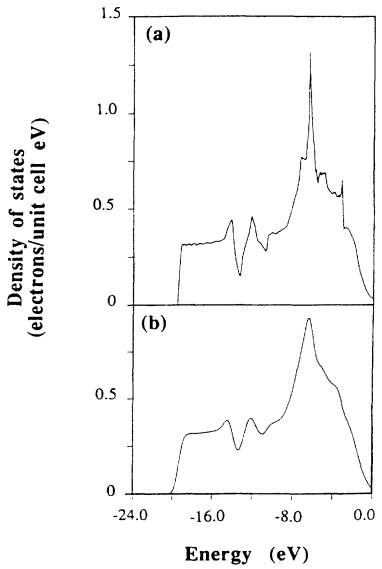

FIG. 4. (a) Theoretical density of states (DOS) of simple hexagonal graphite (b) and with 0.5-eV Gaussian smoothing.

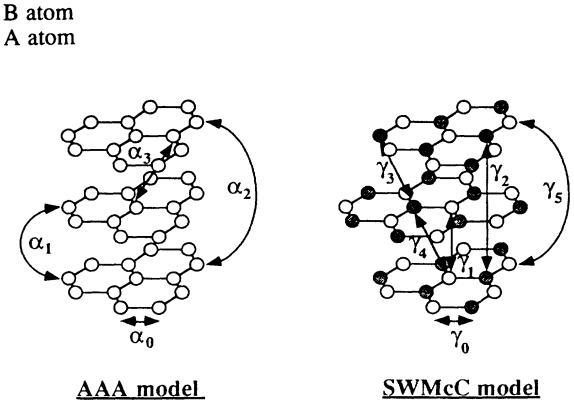

FIG. 5. (a) Graphitical description of the α_i parameters of the *tight-binding* model for simple hexagonal graphite and (b) the γ_i parameters of the SWMcC model. They correspond to overlap integrals between orbitals centered on the atoms connected by arrows.

different carbon atoms inside the plane or from plane to plane. These *tight-binding* parameters are described in Fig. 5 and compared to the SWMcC model parameters.[2]

In the simple hexagonal graphite, all the carbon atoms are equivalent (A atoms). On the contrary, in natural graphite, half of the carbon atoms are A atoms and have a corresponding atom in the plane directly above and below, the whole other half of B atoms have no corresponding atoms in the two nearest-neighbor planes.

B. The *ab initio* Fermi surface

Table II presents the set of parameters α_i for the simple hexagonal graphite calculated by the *ab initio* technique explained before, and compares it with the theoretical and experimental values of the well-known set of γ_i parameters of the *tight-binding* Slonczewski-Weiss-McClure model. The eigenenergies have been calculated starting from the self-consistent density of charge (see Sec. III). A kinetic energy of 36 hartrees has been used corresponding to a number of plane waves which varies between 1220 and 1250. The accuracies obtained for each different value are also presented in Table II.

The comparison with the previous calculations established for the Bernal graphite is as follows. The α_0 parameter, which corresponds to the same interaction as γ_0 in the Bernal structure, leads to the greatest absolute error by comparison with experimental estimations established for γ_0 whose numerical value is 3.16 eV.[22] However, this error is only 20% in relative value which is in the same order of magnitude as the errors in the other parameters. The α_1 parameter corresponding to γ_1 possesses nearly the same numerical value. The γ_2 and γ_3 parameters have no corresponding interaction in the simple hexagonal graphite model. The numerical absolute value obtained for the α_3 parameter is much lower than the corresponding Bernal structure interaction: γ_4. In addition, a negative sign appears in our calculation for this particular structure. Lastly, the α_2 parameter, which corresponds to the γ_5 interaction of the Bernal graphite, is much lower, but its numerical value is not accurate at all.

The linear dispersion relation from point K to point Γ is presented in Figs. 6(a) and 6(b). This figure also shows the band structure of the model for simple hexagonal graphite[12] around the Fermi level for a set of five different directions in an interval of $[-1.5;1.5]$ eV. The comparison with the well-known band structure close to the Fermi level of the SWMcC model[2] is also presented in Figs. 6(c) and 6(d).

For the $ABAB$ stacking [Figs. 6(c) and 6(d)], the *ab initio* calculations reproduced the three well-known bands (ε_1, ε_2, and ε_3 at the K point) of the SWMcC model. ε_1

TABLE II. Values of the *tight-binding* model (Ref. 12) parameters (in eV), of the Fermi energy (in eV) and of the number of free carriers (in $10^{18}/cm^{-3}$) in simple hexagonal graphite and Bernal structure. The first two columns are results obtained by the same theoretical method. The last column is a collection of the best experimental evaluations relative to natural graphite.

	AAA theoretical	$ABAB$ theoretical	$ABAB$ experimental
	$\alpha_0=2.569\pm0.025$[a]	$\gamma_0=2.598\pm0.015$[b]	$\gamma_0=3.16\pm0.05$[c]
	$\alpha_1=0.361\pm0.020$[a]	$\gamma_1=0.364\pm0.020$[b]	$\gamma_1=0.39\pm0.01$[d]
		$\gamma_2=-0.014\pm0.008$[b]	$\gamma_2=-0.020\pm0.002$[e]
		$\gamma_3=0.319\pm0.020$[b]	$\gamma_3=0.315\pm0.015$[f]
	$\alpha_3=-0.032\pm0.015$[a]	$\gamma_4=0.177\pm0.025$[b]	$\gamma_4=0.044\pm0.024$[g]
	$\alpha_2=0.013\pm0.014$[a]	$\gamma_5=0.036\pm0.013$[b]	$\gamma_5=0.038\pm0.005$[d]
		$\Delta=-0.026\pm0.010$[b]	$\Delta=-0.008\pm0.002$[c]
E_F	0.013 ± 0.016[a]	-0.013 ± 0.008[b]	-0.024 ± 0.002[g]
n	350 ± 1.0[a]	1.4 ± 0.8[b]	

[a]Present work.
[b]Reference 4.
[c]Reference 22.
[d]A. Misu, E. Mendez, and M. S. Dresselhaus, J. Phys. Soc. Jpn. **47**, 199 (1979).
[e]D. E. Soule, J. W. McClure, and L. B. Smith, Phys. Rev. **134**, A453 (1964).
[f]R. E. Doezema, W. R. Datars, H. Schaber, and A. Van Schyndel, Phys. Rev. B **19**, 4224 (1979).
[g]E. Mendez, A. Misu, and M. S. Dresselhaus, Phys. Rev. B **21**, 827 (1980).

(tenth band) and ε_2 (seventh band) are associated with atoms which have a neighbor in the first-neighbor graphitic plane (A atoms) while ε_3 is degenerate (eighth and ninth bands) and localized on atoms which do not have any neighbors in the first-neighbor graphitic plane (B atoms). Due to the phase reversal, bonding and antibonding states (ε_2 and ε_1, respectively) are degenerate at the H point and throughout the plane KAL. Starting from H, the splitting of these states gradually increases approaching the K point. The degeneracy of the two ε_3 levels is lifted as we move away from the zone edge, and this is indicated on the left-hand side of Figs. 6(c) and 6(d).

For the AAA stacking [cf. Figs. 6(a) and 6(b)], the folded band structure presents two bands similar to ε_1 and ε_2 in the SWMcC model. As all the atoms in simple hexagonal graphite structure possess a neighbor in the first-neighbor graphitic plane, each band in the folded structure is doubly degenerate and the ε_3 flat bands have totally disappeared.

The general form of the theoretical Fermi surface of simple hexagonal graphite is represented in Figs. 7(a) and 7(b) and compared to the Bernal one in Figs. 7(c)–7(f). In accordance to the focused band structures presented in Fig. 6, the Fermi surface of simple hexagonal graphite is composed of a hole pocket centered at the K point and one electron pocket centered at the H point of the Brillouin zone. By contrast, in the Bernal structure, the electron pocket is found around the K point which is the center of a small longer pocket in accordance with the HKH edge. Above and below this pocket, two small pockets of holes are symmetrically situated. The centers of these hole pockets are localized near H.

The inversion in the nature of the carriers localized around the edge of the Brillouin zone is easy to understand if we refer to the models of these two different allotropic forms of graphite. In simple hexagonal graphite, the positive value obtained for the α_1 parameter ($4\alpha_1$ establishes the width of the π bands at the K point) impose

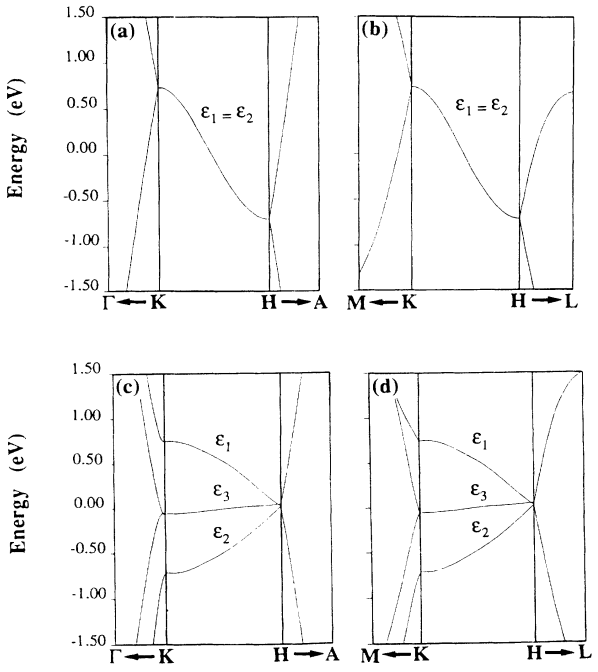

FIG. 6. The band structure of simple hexagonal graphite (a), (b) is detailed around the Fermi level in the interval $[-1.5;1.5]$ eV. The arrows show the direction away from the KH axis. The distances shown are, respectively, $\frac{1}{3}$ of the distance from K to Γ and from H to A, and $\frac{2}{3}$ of the distance from K to M and from H to L. This model (Ref. 12) is compared to the SWMcC model with the corresponding region of the band structure (Ref. 4) (c), (d). Note that the distance between K and H in the Bernal graphite Brillouin zone is half the corresponding K-H distance in the simple hexagonal graphite Brillouin zone, although the scale of our figure does not show it.

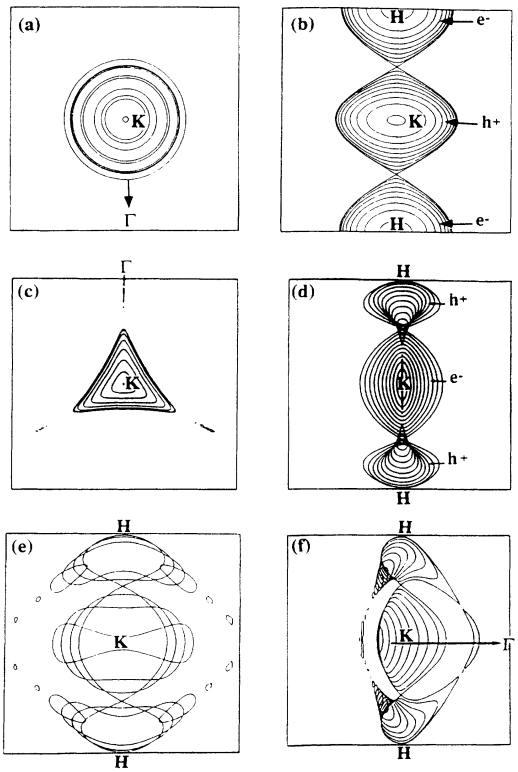

FIG. 7. Cuts in the Fermi surfaces of simple hexagonal graphite (a), (b) and natural graphite (c)–(f) which have been obtained with the theoretical set of α_i and γ_i parameters. (a) Cuts parallel to the AAA stacking graphitic planes. (b) Cuts perpendicular to the AAA stacking graphitic planes and to the $K\Gamma$ direction. (c) Cuts parallel to the $ABAB$ stacking graphitic planes. (d) Cuts perpendicular to the $ABAB$ stacking graphitic planes and to the $K\Gamma$ direction and moved sequentially towards Γ. (e) Cuts perpendicular to the $ABAB$ stacking graphitic planes and to the $K\Gamma$ direction and moved sequentially away from Γ. (f) Cuts perpendicular to the $ABAB$ stacking graphitic planes and performed in the direction perpendicular to the $HK\Gamma$ plane. The between interval is (a) 0.6 a.u., (b) 0.04 a.u., (c) 0.06 a.u., and (d)–(f) 0.004 a.u. Note that the size of the Bernal Fermi surface (c)–(f) perpendicular to the trigonal axis has been scaled by a factor 5 to permit a clear vision of the trigonal warping (Ref. 25).

that the energies of the degenerate bands (last valence band and first conduction band) are higher at the K point than at the H point, while the corresponding domain in natural graphite is limited by the ε_3 degenerate bands (last valence band and first conduction band) where the negative value of the γ_2 parameter ($2|\gamma_2|$ establishes the overlapping magnitude of the π bands) leads to this inversion in the nature of the carriers.

In both cases, these Fermi surfaces include a horizontal mirror plane containing Γ and perpendicular to the HKH edge of the Brillouin zone. Note that the theoretical calculated parameters are such that the limits of the Bernal Fermi surface do not go out of the Brillouin zone and so we do not have any "minority" holes as in experimental Fermi surface.[4]

In the *tight-binding* calculation for simple hexagonal graphite,[12] the effect of the term in $|x|^2$ in the Taylor development, which has not been taken into account in the $\mathbf{k}\cdot\mathbf{p}$ perturbation, is to break the cylindrical symmetry of the Fermi surface, leading to a trigonal symmetry. The simulation of this influence has been represented in Fig. 8. The maximum effect of this term is found to be of the order of 5%. Consequently, it was reasonable to neglect it in that *tight-binding* calculation.[12]

In the Bernal case, retaining only the first term in the corresponding Taylor expansion already leads to a breaking of the cylindrical symmetry to a trigonal one induced by the γ_3 parameter of the SWMcC model [cf. Fig. 7(c)].

C. Interlayer separation effects on the Fermi surface

The effect of the interlayer separation on the *tight-binding* model parameters has been investigated theoretically from the band-structure calculation for various values of layer spacing with no change in the basal plane. This study partially alleviates the lack of experimental data for the c value, in showing what could have been the effect of the use of another lattice parameter. Four values of the lattice constant c in the z direction have been studied, with $(c^*-c)/c^*=0.025$, 0.10, 0.25, and 0.4, where c^* (=3.335 Å) is our calculated value minimizing the total energy as shown in the inset in Fig. 9. Band parameters α_0, α_1, α_2, and α_3 are calculated for these values of c. The results are shown in Fig. 9 for the four parameters. The values of $d\ln\alpha_i/dc$ at c^* are listed in Table III, together with the theoretical and experimental results obtained for the γ_i parameters of Bernal graphite.

The calculation of the c-axis compressibility of simple hexagonal graphite has been performed using the second derivative of the total energy:

$$\frac{d\ln c}{dP}=-\frac{\sqrt{3}a^2}{2c}\left[\frac{\partial^2 E}{\partial c^2}\right]^{-1}=-4.245\times10^{-3}\ \mathrm{GPa}^{-1},$$

and has been compared to the experimental value of the c-axis compressibility[23] of natural graphite which is $-0.027\ \mathrm{GPa}^{-1}$. The AAA c-axis compressibility value is more than six times weaker, due to the particular stacking where all the carbon atoms are directly located on top of each other leading to an increase of the structural rigidity.

According to the *tight-binding* models,[2,12] all the band parameters, except α_0, γ_0, and Δ, are expressed as overlapping integrals between nearest-neighbor (for α_1, α_3, γ_1, γ_4, and γ_3) or next-nearest-neighbor (for α_2, γ_5, and γ_2) layer planes. Therefore, the theoretical result showing their magnitudes increasing with the variation of the interlayer distance was expected. Pressure coefficients of the nearest-neighbor parameters α_1,α_3 and $\gamma_1,\gamma_3,\gamma_4$ are found to be nearly equal with respect to each other. We find that the α_1 parameter changes quadratically versus interplane spacing in the studied region.

The pressure coefficient of the in-plane parameter α_0 is very small, more than one order of magnitude smaller than those of the other parameters. Nothing has changed in the graphitic plane so that they are actually second-order effects.[24] It is to be noted that their signs are positive contrary to the other $d\ln\alpha_i/dc$ and $d\ln\gamma_i/dc$.

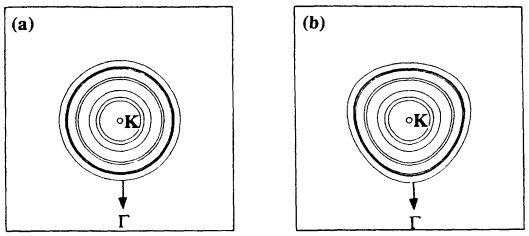

FIG. 8. Cuts in the Fermi surface of simple hexagonal graphite calculated *ab initio* with or without a supplement term $|x|^2$ in the Taylor development of the -$\mathbf{k}\cdot\mathbf{p}$- perturbation established in the tight-binding model (Ref. 12). (a) Cuts parallel to the graphitic planes when there is no $|x|^2$ term in the Taylor development (cylindrical symmetry). (b) Cuts parallel to the graphitic planes when there is an $|x|^2$ term in the Taylor development (trigonal symmetry). The interval is 0.6 a.u.

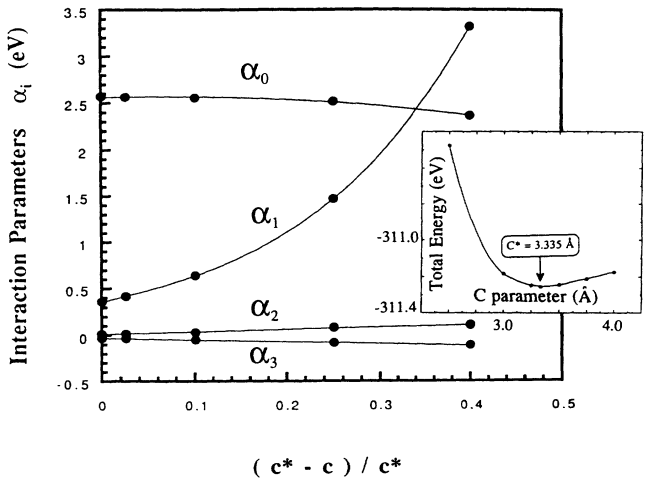

FIG. 9. Band parameters α_i as a function of lattice constant c. The black dots indicate the calculated results. The *ab initio* value of the c parameter (c^*) minimizing the total energy is shown in the inset.

TABLE III. Values of the coefficients $d\ln\alpha_i/dc$ of the band parameters of the two studied modifications of graphite (in Å^{-1}). The first two columns are results obtained by different theoretical methods. The last column is a collection of the best experimental evaluations relative to natural graphite.

	AAA theoretical		*ABAB* theoretical	*ABAB* experimental	
α_0	0.0471[a]	γ_0	0.1664[b]		
α_1	−1.3037[a]	γ_1	−2.0823[b]	−1.2491,[c] −1.9780,[d]	−2.1865[e]
		γ_2	−3.7485[b]	−2.4994,[c] −3.9560,[d]	−1.5620[e]
		γ_3	−1.6663[b]		
α_3	−1.2566[a]	γ_4	−2.2908[b]		
α_2	−0.7387[a]	γ_5	−3.9560[b]		
		Δ	−3.2271[b]	−9.3707,[c]	−23.948[e]

[a]Present work.
[b]Reference 24.
[c]J. R. Anderson, W. J. O'Sullivan, J. E. Schriber, and D. E. Soule, Phys. Rev. **164**, 1038 (1967).
[d]A. I. Likhter and V. V. Kechin, Fiz. Tverd. Tela (Leningrad) **5**, 3066 (1964) [Sov. Phys. Solid State **5**, 2246 (1964)].
[e]K. Noto and T. Tsuzuku, Carbon **12**, 349 (1974).

V. DISCUSSION AND CONCLUSION

In the present paper, the electronic properties of simple hexagonal graphite have been calculated using an *ab initio* technique and related to the electronic properties of Bernal structure when the differences were significant, leading to a qualitative comprehension of the effect of the stacking on these properties. We have successively studied the band structures of these two graphites (that have also been compared to the monolayer case), the DOS of the *AAA* stacking (rather similar to the Bernal structure DOS), and the *tight-binding* parameters for the Fermi surface. An inversion of electrons and holes with respect to Bernal graphite has been explained by studying the influence of the α_1 and γ_2 parameters on these respective surfaces. This result has to be incorporated in rigid-band models when they are used to understand electronic properties of GIC's.

The influence of the interlayer spacing on the band parameters α_i has been calculated from first principles. As is expected, the interlayer-distance dependence of the in-plane parameter (α_0) is found to be very small, and the pressure coefficients relative to the nearest-neighbor parameters (α_1 and α_3) are nearly identical.

ACKNOWLEDGMENTS

We thank Ph. Lambin and J.-P. Vigneron for their interest in this work. One of the authors (J.-C.C.) has benefited from the financial support of the National Fund for Scientific Research (Belgium). This paper presents research results of the Belgian Program of Interuniversity Attraction Poles initiated by the Belgian State–Prime Minister's Office–Science Policy Programming. We also acknowledge the use of the IBM-3090 of the Calculation Center of Louvain-La-Neuve, common project between IBM Belgium and the Catholic University of Louvain-La-Neuve (UCL).

[1]P. R. Wallace, Phys. Rev. **71**, 622 (1947).
[2]J. C. Slonczewski and P. R. Weiss, Phys. Rev. **99**, 636(A) (1955); **109**, 272 (1958); J. W. McClure, *ibid.* **108**, 612 (1957).
[3]See references in M. S. Dresselhaus, G. Dresselhaus, K. Sugihara, I. L. Spain, and H. A. Goldberg, *Graphite Fibers and Filaments,* Springer Series in Materials Science Vol. 5 (Springer-Verlag, Berlin, 1988); N. B. Brandt, S. M. Chudinov, and Ya. G. Ponomarev, *Semimetals. Graphite and its Compounds,* Vol. 20.1 of *Modern Problems in Condensed Matter Sciences* (North-Holland, Amsterdam, 1988).
[4]J.-C. Charlier, X. Gonze, and J.-P. Michenaud, Phys. Rev. B **43**, 4579 (1991).
[5]See, for example, F. Bassani and G. Pastori Parravicini, Nuovo Cimento B **50**, 95 (1967); G. S. Painter and D. E. Ellis, Phys. Rev. B **1**, 4747 (1970), and references therein.
[6]J. D. Bernal, Proc. R. Soc. London Ser. A **106**, 749 (1924).
[7]R. R. Haering, Can. J. Phys. **36**, 352 (1958).
[8]L. Samuelson and I. P. Batra, J. Phys. C **13**, 5105 (1980).
[9]J. Robertson, Adv. Phys. **35**, 317 (1986); S. Mrozowski, Phys. Rev. **77**, 838 (1950); **85**, 609 (1952); **86**, 1056 (1952): P. Nozières, *ibid.* **109**, 1510 (1958); A. Marchand, Carbon **1**, 75 (1963); C. A. Klein, J. Appl. Phys. **33**, 3338 (1962); A. Pacault and A. Marchand, C. R. Acad. Sci. Paris **241**, 489 (1955); A. Marchand, Ann. Chimie **13** (2), 469 (1957); V. Bayot, L. Piraux, J.-P. Michenaud, J.-P. Issi, M. Lelaurain, and A. Moore, Phys. Rev. B **41**, 11 770 (1990); see references in M. S. Dresselhaus, G. Dresselhaus, K. Sugihara, I. L. Spain, and H. A. Goldberg, *Graphite Fibers and Filaments,* Springer Series in Materials Science Vol. 5 (Springer-Verlag, Berlin, 1988).
[10]S. Fahy, S. G. Louie, and M. L. Cohen, Phys. Rev. B **34**, 1191 (1986); **35**, 7623 (1987).
[11]H. Nagayoshi, K. Nakao, and Y. Uemura, J. Phys. Soc. Jpn. **41**, 1480 (1976); R. C. Tatar and S. Rabii, Phys. Rev. B **25**, 4126 (1982); N. A. Holzwarth, S. G. Louie, and S. Rabii, *ibid.* **26**, 5382 (1982); M. Posternak, A. Baldereschi, A. J. Freeman, E. Wimmer, and M. Weinert, Phys. Rev. Lett. **50**, 761 (1983); M. T. Yin and M. L. Cohen, Phys. Rev. B **29**,

6996 (1984); H. J. F. Jansen and A. J. Freeman, *ibid.* **35**, 8207 (1987); D. Tomanek, R. M. Wentzcovitch, S. G. Louie, and M. L. Cohen, *ibid.* **37**, 3134 (1988).

[12]J.-C. Charlier, J.-P. Michenaud, X. Gonze, and J.-P. Vigneron, Phys. Rev. B **44**, 13 237 (1991).

[13]J.-C. Charlier, J.-P. Michenaud, and Ph. Lambin, following paper, Phys. Rev. B **46**, 4540 (1992); S. Flandrois (private communication).

[14]H. W. Kroto, J. R. Heath, S. C. O'Brien, R. F. Curl, and R. E. Smalley, Nature **318**, 162 (1986); H. W. Kroto, Science **242**, 1139 (1988); R. F. Curl and R. E. Smalley, *ibid.* **242**, 1017 (1988); W. Kratschmer, L. D. Lamb, K. Fostiropoulos, and D. R. Huffman, Nature **347**, 354 (1991).

[15]P. Hohenberg and W. Kohn, Phys. Rev. **136**, B864 (1964); W. Kohn and L. J. Sham, *ibid.* **140**, A1133 (1965).

[16]D. M. Ceperley and B. J. Alder, Phys. Rev. Lett. **45**, 566 (1980); J. Perdew and A. Zunger, Phys. Rev. B **23**, 5048 (1981).

[17]J. Ihm, A. Zunger, and M. L. Cohen, J. Phys. C **12**, 4409 (1979).

[18]G. B. Bachelet, D. R. Hamann, and M. Schlüter, Phys. Rev. B **26**, 4199 (1982).

[19]L. P. Bouckaert, R. Smoluchowski, and E. Wigner, Phys. Rev. **50**, 58 (1936).

[20]M. Lax, *Symmetry Principles in Solid State and Molecular Physics* (Wiley Interscience, New York, 1974), pp. 308–311.

[21]G. Lehmann and M. Taut, Phys. Status Solidi B **54**, 469 (1972); Ph. Lambin and J.-P. Vigneron, Phys. Rev. B **29**, 3430 (1984), and references therein.

[22]W. W. Toy, M. S. Dresselhaus, and G. Dresselhaus, Phys. Rev. B **15**, 4077 (1977).

[23]S. G. Kabalkina and L. F. Vereschagin, Dok. Akad. Nauk SSSR **131**, 300 (1960) [Sov. Phys. Dokl. **5**, 373 (1960)].

[24]H. Nagayoshi, J. Phys. Soc. Jpn. **43**, 760 (1977).

[25]The fact that different scales were used for the trigonal axis and the plane perpendicular to it was omitted in the corresponding Fig. 10 of Ref. 4.

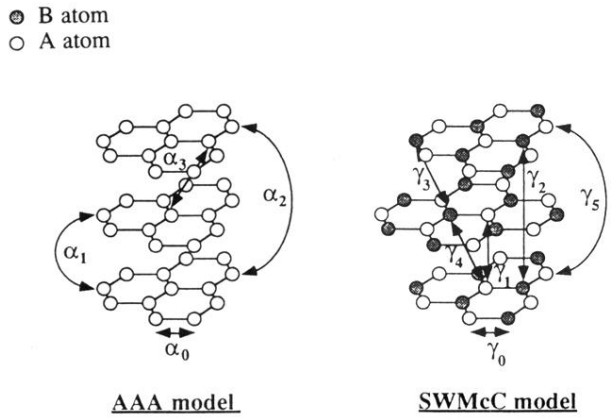

FIG. 5. (a) Graphitical description of the α_i parameters of the *tight-binding* model for simple hexagonal graphite and (b) the γ_i parameters of the SWMcC model. They correspond to overlap integrals between orbitals centered on the atoms connected by arrows.